# Elastic Proton-Proton Scattering: Excitation Functions from 0.45 to 2.5 GeV

Frank Hinterberger for the EDDA Collaboration*

*Helmholtz-Institut f. Strahlen- u. Kernphysik, Univ. Bonn, Nußallee 14-16, D-53115 Bonn*

Excitation functions of the differential cross sections $d\sigma/d\Omega$, analyzing powers $A_N$ and spin correlation parameters $A_{NN}$, $A_{SS}$ and $A_{SL}$ have been measured with internal targets at the Cooler Synchrotron COSY. Data were taken continously during the acceleration and deceleration of the internal beam for kinetic energies between 450 and 2500 MeV and scattering angles $30° \leq \Theta_{cm} \leq 90°$. Details of the experimental method are presented. The results provide excitation functions and angular distributions of high precision and internal consistency. No evidence for narrow structures are found. Upper limits on the coupling of narrow resonances to elastic scattering in the mass range $\sqrt{s} = 2.2 \ldots 2.8$ GeV are deduced. The data have significant impact on phase shift solutions.

# 1 Introduction

Proton-proton elastic scattering experiments [1] are fundamental to the understanding of the NN interaction. At low energies a precise database of differential cross sections and polarization observables has been accumulated. These data are well represented by energy dependent phase shift solutions [2, 3, 4, 5, 6, 7]. Modern phenomenological and meson-theoretical potential models provide excellent descriptions of the data up to the pion threshold [8]. Recent theoretical work based on chiral perturbation theory should also be mentioned in this context [9]. However, the pp scattering data at low energies provide only the understanding of the long- and medium-range parts of the NN interaction.

In view of the repulsive core higher bombarding energies are needed in order to reach small distances ($< 0.8$ fm). It turns out that pp elastic scattering at GeV energies is ideally suited to study the short range part of the NN interaction with high resolution. At 2.5 GeV kinetic energy a four momentum transfer of up to 2.3 GeV/c is reached corresponding to spatial resolutions of less than 0.15 fm. Elastic pp scattering at those energies provides a sharp focus on the role of the $\omega$-meson and other heavy meson exchanges. Apart from the true meson-exchange genuinely new processes might occur at small distances involving the dynamics of the quark-gluon constituents. A related problem is the nature of the repulsive core.

*F. Bauer[b], J. Bisplinghoff[a], K. Büßer[b], M. Busch[a], T. Colberg[b], L. Demirörs[b], C. Dahl[a], P.D. Eversheim[a], O. Eyser[b], O. Felden[c], R. Gebel[c], J. Greiff[b], F. Hinterberger[a], E. Jonas[b], H. Krause[b], C. Lehmann[b], J. Lindlein[b], R. Maier[c], A. Meinerzhagen[a], C. Pauli[b], D. Prasuhn[c], H. Rohdjeß[a], D. Rosendaal[a], P. von Rossen[c], N. Schirm[b], W. Scobel[b], K. Ulbrich[a], E. Weise[a], T. Wolf[b], and R. Ziegler[a] (a) Helmholtz-Institut für Strahlen- und Kernphysik, Universität Bonn, Germany, (b) Institut für Experimentalphysik, Universität Hamburg, Germany, (c) Institut für Kernphysik, Forschungszentrum Jülich, Germany

Another unsettled issue related to the quark-gluon dynamics is the question of existence or nonexistence of dibaryons. Various QCD inspired models predict dibaryonic resonances with c.m. resonance energies $E_R$ ranging between 2.1 and 2.9 GeV. Not any resonance has been observed so far [10]. Excitation functions of differential cross sections, analyzing powers and spin correlation parameters, i.e. cross sections depending on the relative spin orientation of the two incoming protons, provide an especially sensitive test for dibaryonic resonances that may show up in the elastic channel due to the interference between resonant and nonresonant amplitudes.

Closer inspection of the world data set at about 1995 showed that the vast majority of data was below 800 MeV kinetic energy. Above 1200 MeV, the experimental data base was rather poor and there were inconsistencies and normalization errors in the angular distributions measured at different discrete energies. In addition, energy dependent structures had been observed in certain spin observables [11]. The available data allowed to do a Phase-Shift Analysis (PSA) unambiguously up to about 1 GeV [2, 3, 4, 5, 7]. At higher energies, experimental data of sufficient quality and density were not available to determine the increased number of partial waves, leading to serious discrepancies between phase-shift solutions of different groups [7, 12] above 1.2 GeV. A model independent Direct Reconstruction of the Scattering Amplitudes (DRSA) by the Saclay-Geneva group [12] has not solved this problem. The remaining ambiguities allow different PSA solutions.

Therefore, the EDDA experiment at the cooler synchrotron COSY was concieved to provide data of sufficient quality and density. The aim of the experiment is to measure excitation functions of the elastic proton-proton scattering over a wide energy range up to 2.5 GeV in fine energy steps and with a high relative accuracy. Both for a phase shift analysis as such and for its use in identifying central, spin-orbit, spin-spin and spin-tensor forces, it is mandatory to measure not only spin-averaged cross sections, but also spin observables such as analyzing powers $A_N$ and spin correlation coefficients $A_{NN}$, $A_{SS}$ and $A_{SL}$ as a function of the energy. Precise and consistent data are needed both for the improvement and extension of PSA solutions and the development of new theoretical approaches. Until now, only a few relativistic meson exchange models have been extended beyond the pion threshold up to about 1 GeV [8].

In this paper the experimental methods and the results of the EDDA experiment are presented. In the discussion, the impact of the new data on the PSA and the DRSA is shown. The excitation functions allow also to deduce upper limits on the coupling of narrow resonances to the elastic channel in the mass range $\sqrt{s} = 2.2 \ldots 2.8$ GeV.

# 2 Experimental Technique

The EDDA experiment [13, 14, 15] is designed to measure excitation functions of the elastic proton-proton scattering with a high energy resolution over a wide energy range. To this end EDDA was concieved as an internal target experiment in the cooler synchrotron COSY [16]. Data collection proceeds during synchrotron acceleration in a multi-pass technique, so that a full excitation function is measured in each acceleration cycle. Statistical accuracy is obtained by averaging over many cycles. This technique requires (and has demonstrated) a very stable and reproducable operation of COSY. Using the internal recirculating COSY beam has the additional benefit that the luminosities are high enough for measurements with a polarized atomic beam target [13].

In *phase 1*, unpolarized differential cross sections were measured using 4 $\mu$m $\times$ 5 $\mu$m $CH_2$ fiber targets and 5 $\mu$m diameter C fiber targets for background subtraction. In *phase 2*, the analyzing powers $A_N$ were measured as a function of energy using a polarized atomic beam target and a unpolarized proton beam. In *phase 3*, the polarization correlation parameters $A_{NN}$, $A_{SS}$ and $A_{SL}$ were measured as a function of energy using a polarized atomic beam target and a polarized proton beam.

The EDDA detector (Fig. 1) provides large solid angle coverage in a cylindrical geometry and a fast and efficient trigger on low multiplicity events of a given kinematic signature. Elastic events are identified by (i) coplanarity with the beam ($\varphi_1 - \varphi_2 = 180°$) and (ii) the elastic scattering kinematics imposing $\tan\Theta_1 \cdot \tan\Theta_2 = 2m_pc^2/(2m_pc^2+T_p)$. These conditions are employed – with different degrees of stringency – both in triggering and in event identification during off-line analysis.

The EDDA detector consists of two cylindrical double layers covering 30° to 150° in $\Theta_{cm}$ for the elastic pp channel and about 85 % of the full solid angle. The inner layers HELIX are composed of scintillating fibers which are helically wound in opposing directions and connected to 16-channel multianode photomultipliers at backward angles. They are not required for measuring spin-averaged

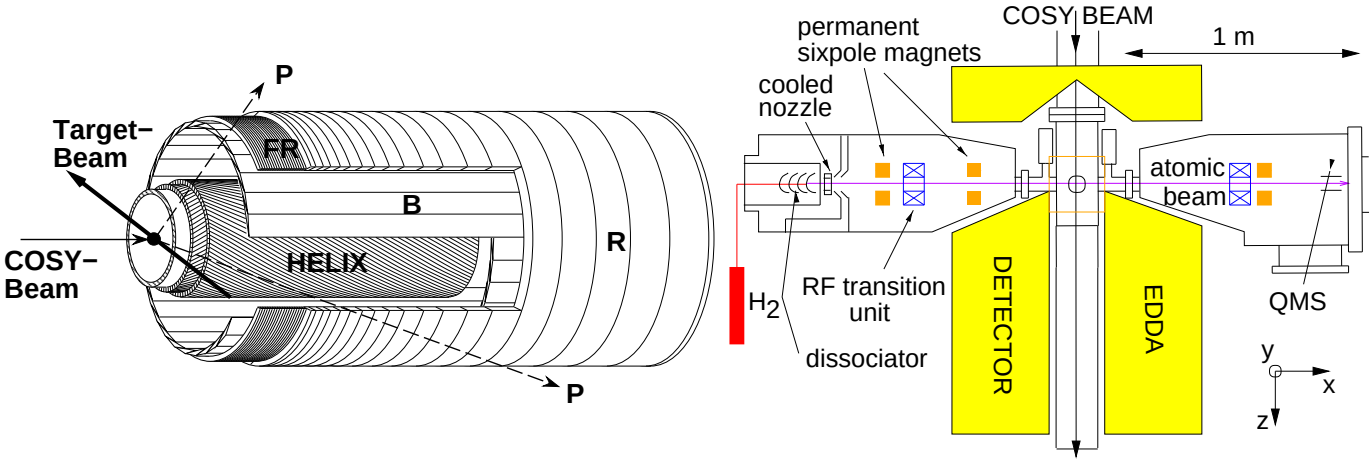


Figure 1: Scheme of the EDDA detector (left) and its combination with the polarized atomic beam target (right). The direction normal to the accelerator plane is denoted y.

cross sections with a $CH_2$ fiber target, but are essential for measuring spin observables with the polarized atomic beam target, as they provide for vertex reconstruction. The outer layers consist of 32 scintillator bars B which are running parallel to the beam axis and which are read out at both ends. They are surrounded by scintillator semi-rings R. The semi-rings FR close to the target are made from scintillating fibers. The scintillator cross sections are designed so that each particle traversing the outer layers produces a signal in two neighbouring bars and rings. Analysis of the fractional light output is used to determine the angles of incidence much more accurately (by a factor of 5) than would be possible on the basis of detector granularity alone. The resulting polar and azimuthal FWHM angle resolution is about 1° and 1.5°, respectively. Combined with the spatial resolution of the 2.5 mm scintillating fibers, this provides a vertex reconstruction with a $1\sigma$ resolution of less than 1 mm in the $x$-, $y$- and $z$-direction. Details are given in [17, 18].

A crucial point of the differential cross section measurements was the luminosity monitor. Relative normalization as a function of momentum was accomplished by measuring (i) the secondary electron current emanating from the fiber target and (ii) the $\delta$-electrons from the elastic proton-electron scattering. The $CH_2$ fiber targets were covered by a 20 $\mu$g/cm$^2$ Aluminum film in order to make them electrically conducting. The secondary electron current scales as the energy deposited into the target fiber. It is proportional to the restricted energy loss rate. The $\delta$-electrons were measured at $\Theta = 40°$ using four silicon detectors located in a left-right, up-down symmetrical arrangement behind thin windows in the beam pipe. The $\delta$-electron rate scales as the Rosenbluth cross section. The two methods give the same relative normalization within 3 % for all beam energies. Absolute normalization is established at 1455 MeV/c with reference to the angular distribution measured by Simon et al. [19] with 1% total uncertainty.

The polarized atomic beam target [20] is shown schematically on the right side of Fig. 1. The polarized hydrogen atoms are prepared using an atomic beam source with dissociator, cooled nozzle, permanent sextupole magnets and rf-transition units. In the beam dump the polarization is continuously monitored using a Breit-Rabi polarimeter. Preparing a polarized atomic beam in a pure hyperfine state yields a peak polarization of 85 %, and an effective target density of about $2{\cdot}10^{11}$ atoms/cm$^2$. The width at the target location is $\sim$12 mm (FWHM). The spin direction is provided by a weak magnetic holding field (1 mT) which can be chosen arbitrarily from cycle to cycle.

The analyzing power excitation functions were taken not only during the acceleration but also during the deceleration of the COSY beam. The direction of the target polarization was changed from cycle to cycle between $\pm x$ and $\pm y$ thus allowing a proper spin flip correction of false asymmetries [21]. Since the polarization of the target is constant during the acceleration and deceleration of the beam (time period $\sim$20 s) a high relative accuracy can be achieved provided the overlap between beam and target can be kept constant. This condition was ideally fulfilled during the measurements. The

COSY accelerator was adjusted such that the vertical beam position and beam width in the target region stayed constant during acceleration and deceleration and the COSY beam (FWHM 6 mm) was centered on the much wider polarized target beam (FWHM 12 mm). The absolute calibration is established with reference to angular distributions measured at 1458 MeV/c [22].

The spin correlation parameters $A_{NN}$, $A_{SS}$ and $A_{SL}$ are measured with a polarized beam and a polarized target. The direction of the target polarization was switched from cycle to cycle to one of six possible directions ±x, ±y, and ±z. In addition the beam polarization was regularly switched between ±y. The spin correlation parameters $A_{NN}$, $A_{SS}$ and $A_{SL}$ describe the deviation of the cross section from the spin-averaged value for the spin of beam and target protons oriented longitudinal to the beam (L) or normal (N) to or sideways (S) in the scattering plane. The scattering rate for each spin combination yields characteristic modulations with the azimuthal angle. With beam intensities ranging from $3 \cdot 10^9$ to $1.5 \cdot 10^{10}$ protons stored we achieved luminosities in the $(1-5) \cdot 10^{27}/(\mathrm{cm}^2\mathrm{s})$ range. We took data during acceleration and at nine evenly spaced flattop-momenta between 2.1 and 3.3 GeV/c. This allows to cover the low (acceleration) and high (flattop) energy region with sufficient statistical accuracy. The spin correlation parameters as well as beam and target polarizations are extracted either by calculating count rate asymmetries [21, 23] which cancel the influence of detector efficiencies to first order, or by standard $\chi^2$ minimization techniques. Both methods yield consistent results. The overall normalization of the target and beam polarizations is fixed with reference to the EDDA analyzing power data [15].

# 3 Results

## 3.1 Differential Cross Sections

Excitation functions of the unpolarized differential cross sections were taken with $CH_2$ and C fiber targets and the outer detector shell alone [14]. Four out of 28 excitation functions [14] are shown on the left side of Fig. 2. On the basis of those new EDDA data and the data of the NN Program at SATURNE [24] Arndt and coworkers were able to extend their phase shift analysis from 1600 MeV (2360 MeV/c) up to 2500 MeV (3300 MeV/c) which is shown as solid curves [6]. The dashed curves are solutions from 1994. All excitation functions show a smooth dependence on beam momentum.

## 3.2 Analyzing Powers

Analyzing power excitation functions in the momentum range 1.0 – 3.3 GeV/c (kinetic energy range 0.45 – 2.5 GeV) are shown on the right side of Fig. 2 and compared to recent phase shift solutions. The data are grouped in ($\Delta\Theta = 4°$, $\Delta$p = 30 MeV/c) wide bins. The dahed curves are calculated using

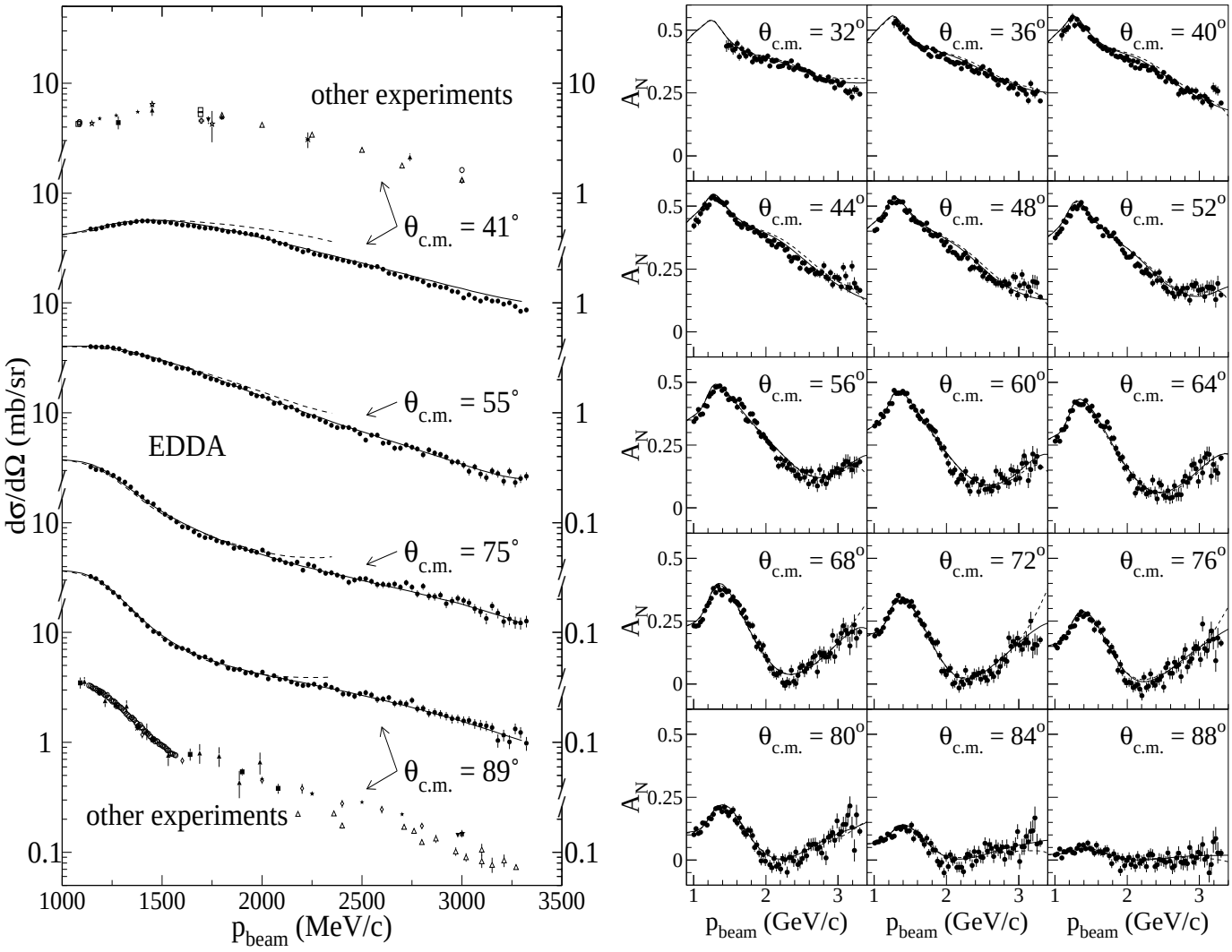


Figure 2: Left: Differential cross section excitation functions for elastic pp scattering at four out of 28 scattering angles. The solid (dashed) curves are from the SM97 (SM94) phase shift analysis [6]. Right: Analyzing power excitation functions for elastic pp scattering in the kinetic energy range 0.45 – 2.5 GeV ($p_{beam}$=1.0 – 3.3 GeV/c). The solid curves are recent phase shift solutions SAID FA00 [7], the dashed curves are the solutions SAID SM97 from summer 97 [6].

the phase shift solution SAID SM97 from summer 97. The solid curves represent a more recent phase shift solution FA00 from fall 2000. In this analysis also the new analyzing power data from EDDA were included. The general trend of the excitations functions is reproduced by the recent phase shift solutions but there are still some systematic deviations at higher momenta.

## 3.3 Spin-Correlation Parameters

The data analysis of phase 3 is almost finalized. Preliminary data on the spin correlation parameters $A_{NN}$, $A_{SS}$ and $A_{SL}$ are shown in Fig. 3 in comparison to phase shift predictions of SAID [7] (SM00, solid) and the Saclay-Geneva [12] (dashed line) analysis. On the left excitation functions of spin correlation parameters at $\theta_{\text{c.m.}} = 47.5°$ are shown. Here, open and closed symbols distinguish data

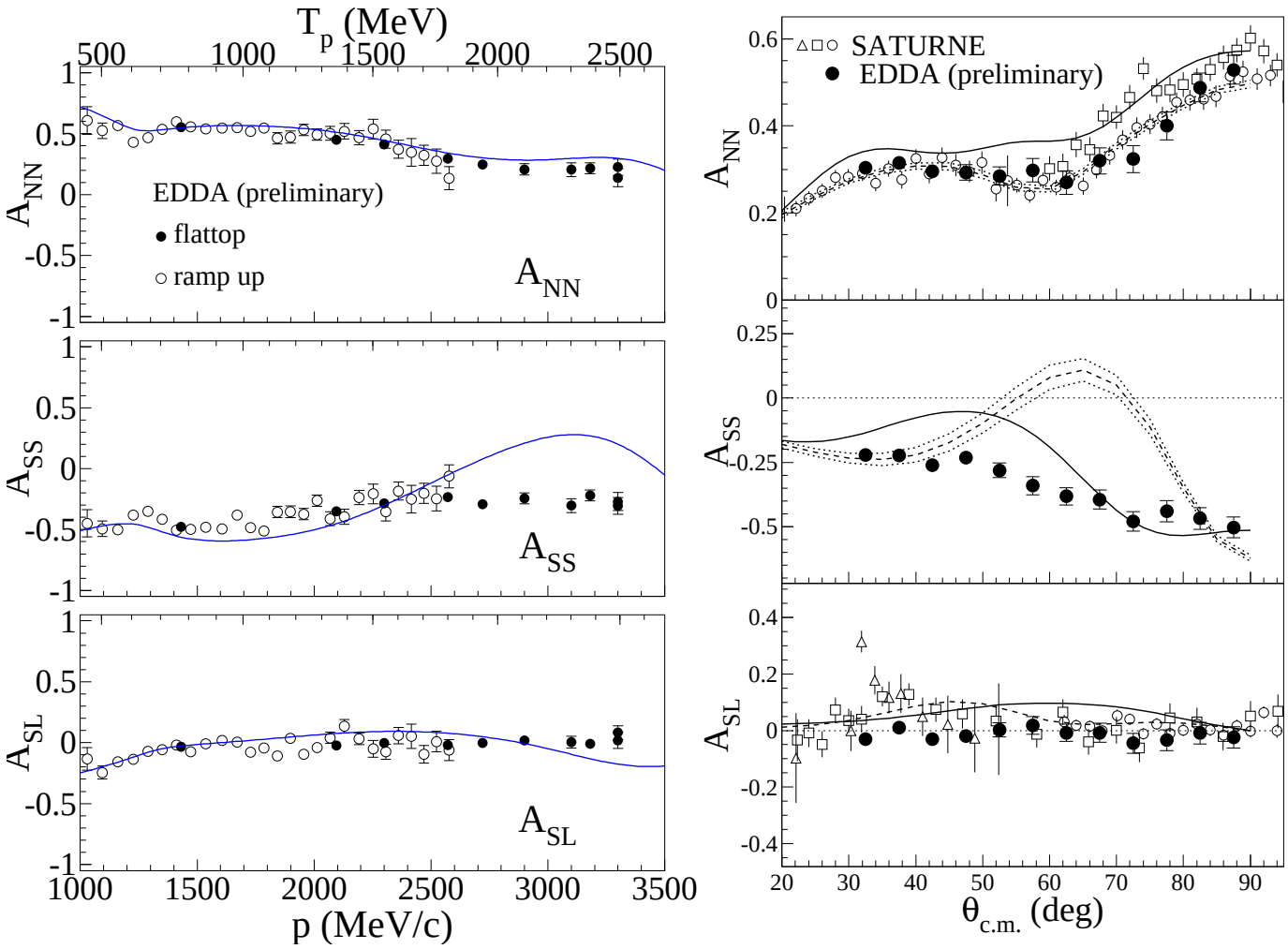


Figure 3: Excitation functions at $\theta_{\mathrm{c.m.}} = 47.5°$ (left) and angular distributions at $T_p = 1800$ MeV (right) of spin correlation parameters $A_{NN}$, $A_{SS}$ , and $A_{SL}$ in comparison to phase shift predictions of SAID [7] (SM00, solid) and the Saclay-Geneva [12] (dashed line) analysis. On the left, closed (open) symbols distinguish data points measured at the flattop (during acceleration) of the COSY machine cycle. On the right, data from SATURNE [24] are shown as open symbols.

points measured during the acceleration and the flattop of the COSY machine cycle. On the right angular distributions at the fixed energy $T_p = 1800$ MeV are shown. Previous measurements of spin correlation parameters at fixed energies were mainly done at SATURNE [24] (open symbols on the right side). In comparison, our new data on $A_{NN}$ is consistent at all energies. However, we find values for $A_{SL}$ more or less compatible with zero at all angles and do not confirm excursions in the angular distributions as observed in the SATURNE data.

The observable $A_{SS}$ has not been measured before above 800 MeV. The new data disagree strikingly with different PSA solutions. It will be interesting to see to what extent the new spin correlation data on $A_{SS}$ will modify the PSA solutions. As a first step we found [25] that the addition of our data to the world database removes some of the ambiguities in the direct reconstruction of the scattering amplitudes (DRSA) found in [12].

# 4 Upper Limits on Resonance Contributions

The excitation functions of the differential cross sections and analyzing powers have shown no evidence for narrow resonances. Therefore, upper limits for the elasticities $\Gamma_{el}/\Gamma$ of hypothetical narrow resonances have been deduced from the smooth excitation functions. To this end a Breit-Wigner term is introduced into the scattering matrix element of a resonating partial wave $(L, J)$,

$$S_{LJ} = \eta_{LJ} e^{2i\delta_{LJ}} - i e^{2i\phi_R} \eta_{LJ} \frac{\Gamma_{el}}{\Gamma} \frac{\Gamma}{E - E_R + i\Gamma/2}. \quad (1)$$

Here, $\eta_{LJ} e^{2i\delta_{LJ}}$ is the nonresonant background amplitude, $\Gamma_{el}$ the partial elastic width, $\Gamma$ the total

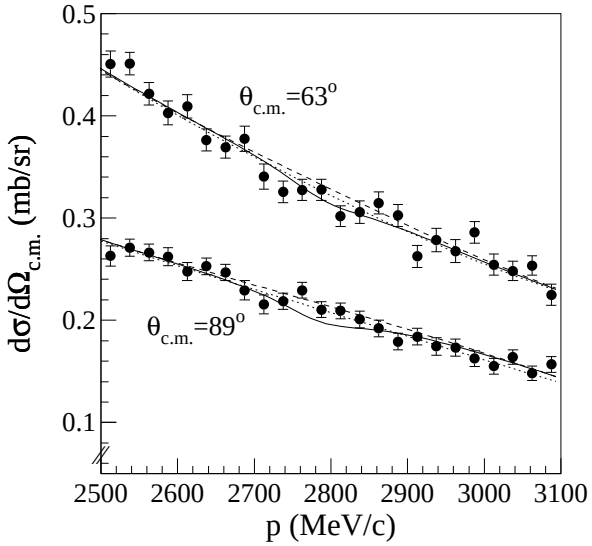


Figure 4: Differential cross sections at two out of 28 scattering angles in comparison to PSA solutions. The best fit, with (without) a $^1S_0$ resonance at $E_R = 2.7$ GeV, $\Gamma = 50$ MeV and $\Gamma_{el}/\Gamma = 0.043$, excluded with 99% CL by the data is shown as the solid (dashed) line. The dotted line shows the nonresonant background as described by the PSA in the presence of the resonance.

width, $E_R$ the resonance energy and $\phi_R$ the phase of the resonance. The interference between the resonant and nonresonant amplitudes determines the size of a resonance excursion in the excitation functions. The elasticity $\Gamma_{el}/\Gamma$ is a measure of the coupling between the resonance and the nonresonant continuum. In order to establish a null-hypothesis the EDDA data have been fitted by a special energy dependent PSA analysis along Ref. [6]. The fitted phase shift parameters have been used for the nonresonant background amplitudes and the compatibility of a narrow resonance with the data has been tested quantitatively [26]. This can be done as long as the energy dependence assumed in the PSA is slowly varying with energy as compared to the resonance width to be tested. In the test calculations the resonance parameters $E_R$, $\Gamma$ and $\phi_R$ were varied systematically in the range $E_R = 2200 \ldots 2800$ MeV, $\Gamma = 10 \ldots 100$ MeV and $\phi_R = 0° \ldots 360°$. The hypothesis of the existence of a resonance in a partial wave was tested by gradually increasing the partial elastic width $\Gamma_{el}$ until

the resonance was excluded withh 99% confidence level (CL) by a $\chi^2$-test based on the EDDA data. For the unknown phase $\phi_R$ the value giving the largest $\Gamma_{el}/\Gamma$ excluded was chosen. An example – corresponding to a $^1S_0$-resonance predicted in Ref. [27] – is shown in Fig. 4. Typical upper limits of $\Gamma_{el}/\Gamma$ for the five lowest uncoupled partial waves are 0.08 for $^1S_0$, 0.04 for $^2D_2$, 0.10 for $^3P_0$, 0.03 for $^3P_1$ and 0.05 for $^3F_3$. The EDDA data, i.e. the differential cross section and analyzing power data, exclude a sizeable coupling of resonances, like dibaryons, to the elastic proton-proton channel in the parameter space covered.

# 5 Summary and Conclusions

The principle of measuring excitation functions with internal targets during acceleration and deceleration works well. On the basis of the new EDDA data on $d\sigma/d\Omega$ the energy dependent PSA solutions [6] have been extended from 1600 to 2500 MeV. The analyzing power excitation functions provide a new polarization standard in the GeV region. The spin correlation data on $A_{SS}$ which disagree strikingly with existing PSA solutions will have a major impact on forthcoming PSA solutions. The smooth excitation functions allow to deduce sharp upper limits for the occurence of narrow resonances in the elastic channel.

The excellent support by the COSY accelerator team is warmly acknowledged. We are indebted to Prof. R. Arndt for providing us and helping with the PSA-software.

# References

[1] C. Lechanoine-Leluc and F. Lehar, Rev. Mod. Phys. 65 (1993) 47.

[2] V. G. J. Stoks et al., Phys. Rev. **C48**, (1993) 792.

[3] J. Bystricky, C. Lechanoine-LeLuc, and F. Lehar, J. Phys. (Paris) **48**, (1987) 199.

[4] J. Bystricky, C. Lechanoine-LeLuc, and F. Lehar, J. Phys. (Paris) **51**, (1990) 2747.

[5] J. Nagata, H. Yoshino, and M. Matsuda, Prog. Theor. Phys. **95**, (1996) 691.

[6] R. A. Arndt et al., Phys. Rev. **C56**, (1997) 3005.

[7] R. A. Arndt, I. I. Strakovsky, and R. L. Workman, Phys. Rev. C **62**, (2000) 34005.

[8] R. Machleidt and I. Slaus, J. Phys. **G27**, (2001) R69, and references herein.

[9] P. F. Bedaque and U. van Kolck, Ann. Rev. Nucl. Part. Sci. **52**, (2002) 339.

[10] K. K. Seth, Proc. "Baryon-Baryon Interaction and Dibaryonic Systems", Bad Honnef, 1988, p. 41.

[11] J. Ball et al., Phys. Lett. B320 (1994) 206.

[12] J. Bystricky, F. Lehar, and C. Lechanoine-LeLuc, Eur. Phys. J. **C4**, (1998) 607.

[13] J. Bisplinghoff and F. Hinterberger, Particle Production Near Threshold, AIP Conf. Proc. 221 (1991) 312; W. Scobel, Phys. Scr. 48 (1993) 92; H. Rohdjeß, Proc. Int. Conf. on Physics with GeV-Particle Beams, Jülich, 1994, World Scientific (1995) 334.

[14] D. Albers et al., (EDDA) Phys. Rev. Lett. 78 (1997) 1652.

[15] M. Altmeier et al., (EDDA) Phys. Rev. Lett. 85 (2000) 1819.

[16] R. Maier, Nucl. Instr. and Meth. in Phys. Res. A 390 (1997) 1.

[17] J. Bisplinghoff et al., (EDDA) Nucl. Instr. and Meth. A 329 (1993) 151.

[18] M. Altmeier et al., (EDDA) Nucl. Instr. and Meth. in Phys. Res. A431 (1999) 428.

[19] A.J. Simon et al., Phys. Rev. C48 (1993) 662; C53 (1996) 30.

[20] P.D. Eversheim, Nucl. Phys. A626 (1996) 117c.

[21] G. G. Ohlsen and P.W. Keaton Jr., Nucl. Instr. and Meth. **109**, (1973) 41.

[22] M.W. McNaughton et al., Phys. Rev. C23 (1981) 1128.

[23] F. Bauer, Ph.D. thesis, Universität Hamburg, 2001.

[24] J. Ball et al., CTU Reports **4**, (2000) 3.

[25] F. Bauer et al., (2002), nucl-ex/0209006.

[26] H. Rohdjess, Habilitationsschrift, Universität Bonn, 2000.

[27] P. González, P. LaFrance and E.L. Lomon, Phys. Rev. D35 (1987) 2142.